Astronomy & Astrophysics manuscript no. IGR˙to˙sub˙to˙arxiv
July 27, 2011

The masses of the neutron and donor star in the high-mass X-ray binary IGR J18027-2016 ⋆
(Research Note)

A.B. Mason[1], A.J. Norton[1], J.S. Clark[1], I. Negueruela[2], and P. Roche[1,3,4]

[1] Department of Physics & Astronomy, The Open University, Milton Keynes MK7 6AA, UK
[2] Departamento de Física, Ingeniería de Sistemas y Teoría de la Señal, Universidad de Alicante, Apdo. 99, E03080 Alicante, Spain
[3] School of Physics & Astronomy, Cardiff University, The Parade, Cardiff, CF24 3AA, UK.
[4] Division of Earth, Space & Environment, University of Glamorgan, Pontypridd, CF37 1DL, UK.

Received 02 June 2011 / Accepted 02 July 2011

ABSTRACT

Aims. We report near-infrared observations of the supergiant donor to the eclipsing high mass X-ray binary pulsar IGR J18027-2016. We aim to determine its spectral type and measure its radial velocity curve and hence determine the stellar masses of the components.
Methods. ESO/VLT observations of the donor utilising the NIR spectrograph ISAAC were obtained in the H and K bands. The multi-epoch H band spectra were cross-correlated with RV templates in order to determine a radial solution for the system.
Results. The spectral type of the donor was confirmed as B0-1 I. The radial velocity curve constructed has a semi-amplitude of 23.8 ± 3.1 km s^{-1}. Combined with other measured system parameters, a dynamically determined neutron star mass of 1.4 ± 0.2 - 1.6 ± 0.3 $M_\odot$ is found. The mass range of the B0-B1 I donor was 18.6 ± 0.8 - 21.8 ± 2.4 $M_\odot$. These lower and upper limits were obtained under the assumption that the system is viewed edge-on (i = 90° with $\beta = 0.89$) for the lower limit and the donor fills its Roche lobe ($\beta = 1$ with i = 73.1°) for the upper limit respectively.

Key words. binaries:eclipsing - binaries:general - X-rays:binaries - stars:individual:IGR J18027-2016

1. Introduction

The precise nature of the fundamental properties of neutron star (NS) matter has been an on-going field of research for many decades. The physical properties of matter that exist in the extreme densities and pressures found within a NS can be determined by the NS equation of state (EoS). At this juncture however there exist over 100 proposed EoS (Kaper et al. 2006). Only one can be physically valid. Observational data can assist in reducing this number by eliminating contending EoS that place unrealistic constraints on the mass range of observed NSs.
Many EoS predicting the presence of exotic hadronic matter have been ruled out by the recent mass determination of 1.97 ± 0.04 $M_\odot$ for the binary millisecond pulsar (MSP) PSR J1614-2230 (Demorest et al. 2010). In the case of PSR J1614-2230 it is believed that the over-massive NS in this system was created by the accretion of matter whilst being spun-up to become a MSP. Another possible means of high mass NS production may occur where massive progenitors have yielded a high pre-SN core mass. High Mass X-ray Binary systems (HMXBs) are potential testing grounds for this idea as in the majority of cases the progenitor of the NS will be more massive than the donor star we can observe.
The only means of performing unambiguous NS mass determinations in X-ray pulsar binaries is by observing eclipsing binary systems in which we can constrain the inclination angle. There are presently 10 such systems known with 8 in which the NS mass has been calculated (e.g. Mason et al. (2011); Mason et al. (2010); Quaintrell et al. (2003)). In this paper we present an orbital solution from observations of the donor within the HMXB accretion driven pulsar IGR J18027-2016. The mass donor within this system is heavily obscured and reddened. Using near infrared spectroscopy of the donor star we have calculated an orbital solution to measure the mass of each of the components within the system.
IGR J18027-2016 was first detected by *INTEGRAL* in 2003, (Revnivtsev et al. 2004) and was spatially associated with the X-ray pulsar SAX J18027.7-2017 which was discovered serendipitously during observations of the LMXB GX9+1 and found to have a pulse period of 139.6 s (Augello et al. 2003). IGR J18027-2016 has a measured hydrogen column density, N_H = 9.1 ± 0.5 × 10^{22} cm^{-2} (Walter et al. 2006) greatly in excess of the line of sight column density of $N_H = 1.0 \times 10^{22}$ cm^{-2}. This is indicative of intrinsic absorption occurring within the system, with matter from the stellar wind of the donor forming a dense spherical shell around the NS as it is accreted (Hill et al. 2005).
XMM-Newton observations in 2004 narrowed the source position down (with an uncertainty of 4″) to the location RA(2000.0) = $18^h02^m42.0^s$ and Dec = -20°17′18″ (Walter et al. 2006). Using this improved position Masetti et al. (2008) were able to identify the donor as 2MASS J18024194-2017172 (J = 12.7, H = 11.9, K = 11.5).
From timing analysis IGR J18027-2016 was found to have an orbital period of 4.5696 ± 0.0009 days (Hill et al. 2005). The orbit based upon the sinusoidal modulation of pulse arrival times was found to be approximately circular. Using a donor mass-radius relation together with approximations of the Roche lobe radius Hill et al. (2005) proposed that the donor is a 09 - B1 supergiant.

⋆ Based on observations carried out at the European Southern Observatory under programme ID 085.D-0539(A)

Table 1. The phase, radial velocity and telluric standard for each IGR J18027-2016 spectrum.

Mid-point of Observations (UT)	MJD	Phase	Radial velocity / km s^{-1}	Telluric Std
2010 July 13.161	55390.16060	0.073	51.8 ± 9.9	Hip 088201
2010 July 09.017	55386.01693	0.166	76.9 ± 9.9	Hip 089744
2010 April 22.336	55308.34560	0.169	68.4 ± 9.9	RV std
2010 June 07.210	55354.21010	0.205	85.2 ± 9.9	Hip 092931
2010 Aug 10.197	55418.19702	0.208	79.9 ± 9.9	Hip 092322
2010 Sept 06.995	55445.99528	0.291	76.0 ± 9.9	Hip 094859
2010 June 12.252	55359.25220	0.309	69.2 ± 9.9	RV std
2010 June 22.074	55369.07022	0.457	64.8 ± 9.9	RV std
2010 Aug 25.171	55433.17163	0.485	47.7 ± 9.9	Hip 100170
2010 Aug 16.111	55424.11101	0.502	48.6 ± 9.9	Hip 092470
2010 Sept 08.080	55447.07987	0.529	33.4 ± 9.9	Hip 090804
2010 July 29.211	55406.21077	0.585	42.6 ± 9.9	Hip 089384
2010 June 09.095	55356.09537	0.618	37.8 ± 9.9	Hip 083535
2010 May 26.392	55342.39190	0.619	22.7 ± 9.9	RV std
2010 Aug 08.104	55416.10351	0.750	19.9 ± 9.9	Hip 101552
2010 Aug 31.054	55439.05354	0.772	24.2 ± 9.9	Hip 094378
2010 June 19.167	55366.16684	0.822	56.4 ± 9.9	HD 169101
2010 July 08.191	55385.19053	0.985	56.3 ± 9.9	Hip 090978

Optical and NIR spectral analysis of the mass donor performed by Chaty et al. (2008) detected prominent Paschen and Brackett series hydrogen lines in addition to He I and He II lines in emission. Combining their spectroscopy with SED modelling they proposed that the mass donor was an early B supergiant. Obtaining higher resolution spectra in the I and K bands Torrejón et al. (2010) narrowed the spectral type down to B1 Iab - B1 Ib. The short orbital period of IGR J18027-206 of only 4.6 d eliminated the donor being a B1 Iab supergiant, they proposed a classification of B1 Ib for the mass donor lying at a distance of 12.4 kpc.

2. Observations and Data Reduction

Observations were conducted between 2010 May 26th and 2010 Sept. 08th using the NIR spectrograph ISAAC on the VLT in the SW MRes mode utilising a 0.8″ slit width. Although the mass donor in IGR J18027-2016 is relatively faint (H = 11.91) we were able to obtain medium resolution (R ∼ 3000) and high S/N spectra in the H and K_s bands. For the H band multi-epoch science and RV template exposures centred on 1.7 μm were obtained of 2400s and 200s respectively. For the K_s band two science exposures centred on 2.06 and 2.15 μm were taken for a total of 2240s. Reduction was performed using the ISAAC pipeline with OH skylines used to wavelength calibrate the spectra. The resulting data has a count rate less than 10 000 ADU and thus no correction for detector non-linearity was necessary. The RV template observed was Hip 89262, with a known RV of -8 km s^{-1}, close in spectral type to the target (B0.5 Ia) and bright (H ∼ 6.8).

We obtained a dataset containing 18 spectra. Telluric correction was employed to remove atmospheric features from each spectrum. Unfortunately, no telluric standards were obtained for the first four spectra in our dataset (see Table 1). In this case we employed the RV template (which had an airmass close to that of the target) as a telluric standard. In order not to contaminate our target spectrum we first removed any non-telluric spectral lines from the RV template before telluric correction was attempted. The continuum normalised H band spectra comprising our full dataset ordered by phase are shown in Fig. 1.

3. Data Analysis

Using the standard IRAF[1] routine *fxcor*, radial velocities were determined by cross-correlating the region around the He I 1.70 μm absorption line in the 8 science spectra against the same region in the RV template spectra which were obtained shortly after each science exposure. The resulting radial velocities were then corrected to the solar system barycentre and are reported in Table 1. The eccentricity of the system is reported as e $\lesssim$ 0.2 (Augello et al. 2003) and although no precise measurement of the eccentricity is reported, Hill et al. (2005) found sinusoidal modulation from an analysis of pulse arrival times that indicates the NS is in a circular orbit around the mass donor. We have thus fitted the radial velocities of the supergiant donor with a sinusoidal solution, using the ephemeris of Hill et al. (2005) which specifies the epoch of mid-eclipse as

$$T(MJD) = 52168.26(4) + 4.5696(9)N \quad (1)$$

the uncertainties in brackets refer to the last decimal place quoted and N is the cycle number. At the epoch of our observations the accumulated uncertainty in phase is 0.11. We therefore fitted our data with two models, one in which the zero phase is fixed and the other in which we allowed the zero phase to vary as a free parameter.

In our first model we fixed the zero phase and allowed the systemic velocity and RV semi-amplitude to vary as free parameters. Fitting a sinusoid to our data we found the radial velocity semi-amplitude K_O = 24.4 ± 3.2 km s^{-1} and systemic velocity γ = 51.7 ± 2.4 km s^{-1}. To obtain this solution the uncertainties in RV for each data point had to be scaled to ± 9.9 km s^{-1} thus reducing chi-squared to unity.

Alternatively fitting a sinusoid to our data with three free parameters (allowing in this case the zero phase to vary) we found the radial velocity semi-amplitude K_O = 23.8 ± 3.1 km s^{-1}, systemic velocity γ = 52.5 ± 2.4 km s^{-1} and a phase shift of -0.03 ± 0.02. Here the uncertainties were scaled to ± 9.7 km s^{-1}. The best-fit phase offset found is within the accumulated phase uncertainty of the ephemeris. We prefer this fit and use the data

[1] IRAF is distributed by the National Optical Astronomy Observatory, which is operated by the Association of Universities for Research in Astronomy, Inc., under cooperative agreement with the National Science Foundation.

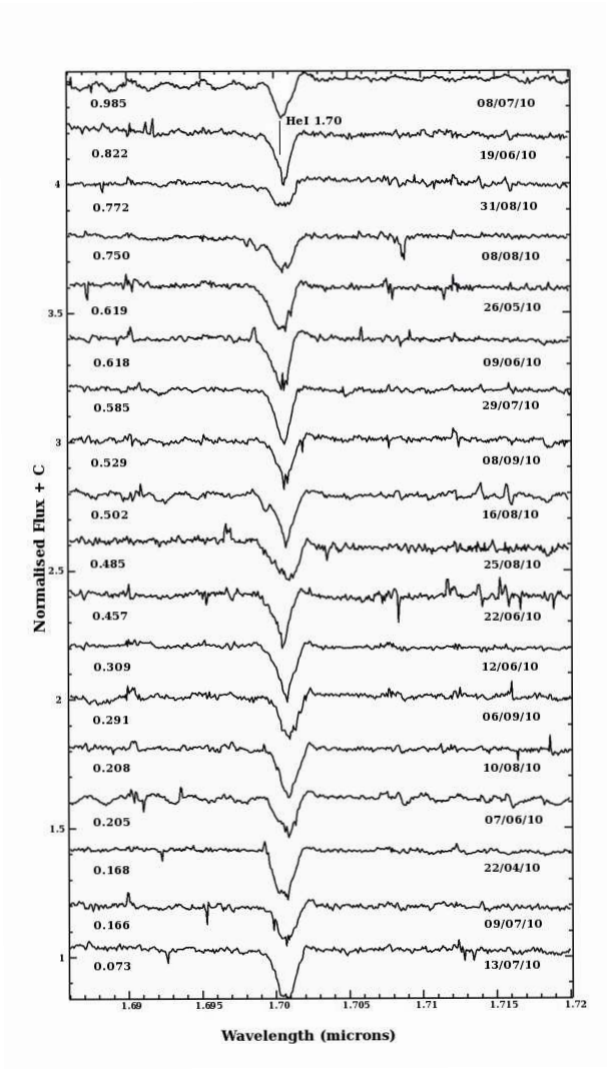

Fig. 1. Continuum normalised H-band spectra centred on He I 1.70 μm of IGR J18027-2016 in order of phase from bottom to top.

from it for our subsequent calculations of the system parameters of IGR J18027-2016. Both fits are shown in Fig 2.

The projected semi-major axis of the neutron star's orbit from X-ray pulse timing delays was measured by Hill et al. (2005) as $a_x \sin i = 68.0 \pm 1$ light seconds. From this, the semi-amplitude of the neutron star's radial velocity may be calculated using

$$a_{\rm X} \sin i = \left(\frac{P}{2\pi}\right) K_{\rm X} \tag{2}$$

for a circular orbit to give $K_{\rm X} = 324.4 \pm 4.7$ km s^{-1}.

To determine the component masses of the system we must first consider the mass ratio of the system q which is equal to the ratio of the semi-amplitudes of the radial velocities for each star

$$q = \frac{M_{\rm X}}{M_{\rm O}} = \frac{K_{\rm O}}{K_{\rm X}} \tag{3}$$

where $M_{\rm X}$ and $M_{\rm O}$ are the masses of the neutron star and supergiant star respectively, and $K_{\rm X}$ and $K_{\rm O}$ are the corresponding

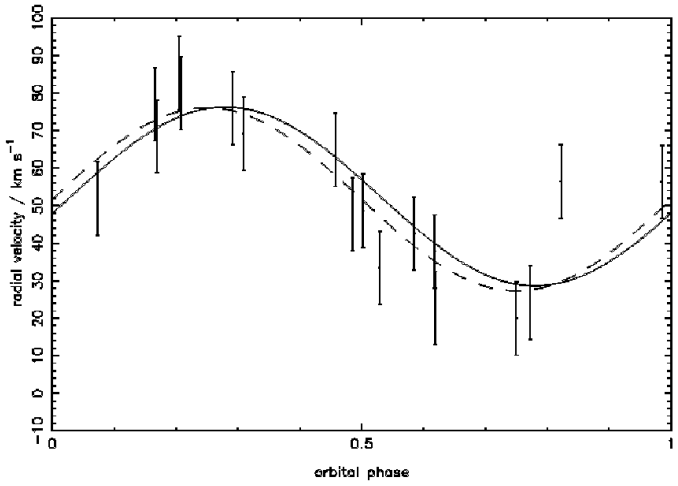

Fig. 2. Radial velocity data for the supergiant mass donor in IGR J18027-2016. The solid line is the best fitting sinusoid with three free parameters, the dashed line is that with a fixed zero phase in line with the published ephemeris. The orbital phase is based upon the ephemeris of Hill et al. (2005).

Table 2. System parameters for IGR J18027-2016.

Parameter	Value		Ref.
Observed			
$a_{\rm X} \sin i$ / lt sec	68 ± 1		[1]
P / d	4.5696 ± 0.0009		[1]
T_{90} / MJD	52168.26 ± 0.04		[1]
e	$\lesssim 0.2$		[2]
$\theta_{\rm e}$ / deg	34.9 ± 4.6		[1]
$K_{\rm O}$ / km s^{-1}	23.8 ± 3.1		[3]
Assumed			
Ω	$= 1$		
Inferred			
$K_{\rm X}$ / km s^{-1}	324.4 ± 4.7		
q	0.073 ± 0.01		
β	1.000	0.893 ± 0.078	
i / deg	73.1 ± 6.3	90.0	
$M_{\rm X}$ / M$_\odot$	1.58 ± 0.27	1.36 ± 0.21	
$M_{\rm O}$ / M$_\odot$	21.8 ± 2.4	18.6 ± 0.8	
a / R$_\odot$	33.1 ± 1.2	31.4 ± 0.5	
$R_{\rm L}$ / R$_\odot$	19.8 ± 0.8	18.8 ± 0.3	
$R_{\rm O}$ / R$_\odot$	19.8 ± 0.7	16.8 ± 1.5	

[1] Hill et al. (2005); [2] Augello et al. (2003)
[3] this paper

semi-amplitudes of their radial velocities. In addition, for circular orbits,

$$M_{\rm O} = \frac{{K_{\rm X}}^3 P}{2\pi G \sin^3 i} (1+q)^2 \tag{4}$$

and similarly

$$M_{\rm X} = \frac{{K_{\rm O}}^3 P}{2\pi G \sin^3 i} \left(1 + \frac{1}{q}\right)^2 \tag{5}$$

where i is the inclination to the plane of the sky and P is the orbital period. The system inclination can be found from the geometric relation

$$\sin i \approx \frac{\left[1 - \beta^2 \left(\frac{R_L}{a}\right)^2\right]^{1/2}}{\cos\ \theta_{\rm e}} \tag{6}$$

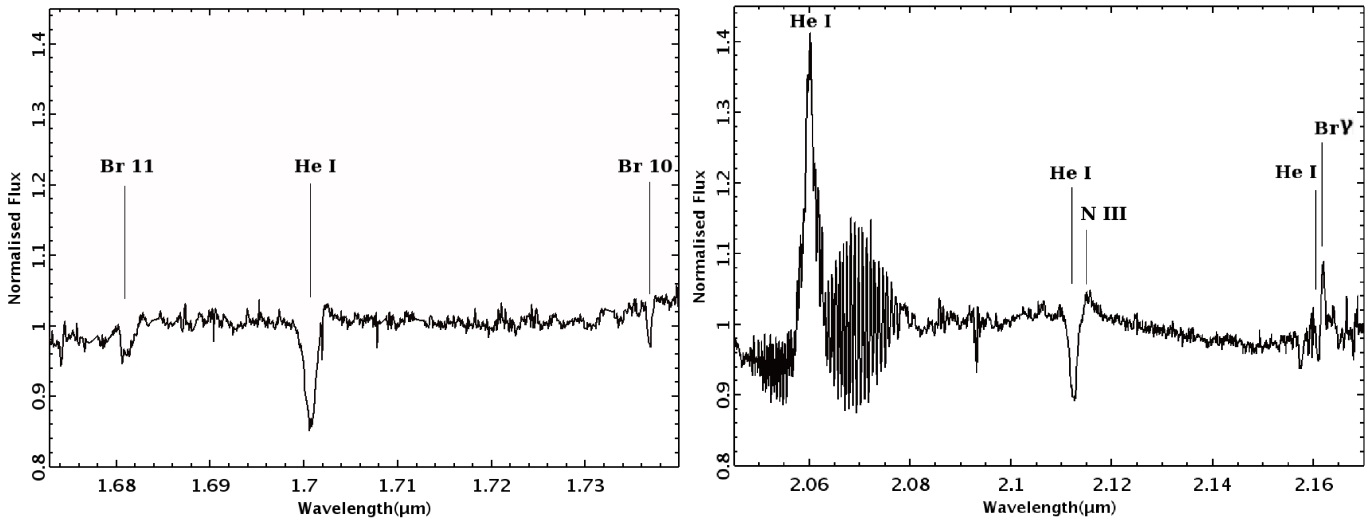

Fig. 3. *Left*: IGR J18027-2016 continuum normalised H band spectrum. *Right*: Continuum normalised K_s band spectrum of IGR J18027-2016.

where θ_e is the eclipse half-angle, R_L is the Roche lobe radius of the supergiant, β is the ratio the supergiant's radius to that of its Roche lobe and a is the separation between the centres of mass of the two stars. The Roche lobe radius may be approximated by

$$\frac{R_L}{a} \approx A + B\log q + C\log^2 q \quad (7)$$

where the constants have been determined by Joss & Rappaport (1984) as

$$A \approx 0.398 - 0.026\Omega^2 + 0.004\Omega^3 \quad (8)$$

$$B \approx -0.264 + 0.052\Omega^2 - 0.015\Omega^3 \quad (9)$$

$$C \approx -0.023 - 0.005\Omega^2 \quad (10)$$

Ω is the ratio of the spin period of the supergiant to its orbital period. We have assumed that the supergiant is close to Roche lobe-filling and will likely be rotating synchronously with the orbit, so $\Omega = 1$, and the eclipse half angle is taken to be $\theta_e = 34.9° \pm 4.6°$ (Hill et al. 2005).

Equations (2) - (10) allow the masses of the two stars to be determined in two limits. First, assuming that the system is viewed edge-on (in which case $i = 90°$) we can find a lower limit to the Roche lobe filling factor β and lower limits to the stellar masses. Secondly, assuming that the supergiant fills its Roche lobe (in which case $\beta = 1$) we can find a lower limit to the system inclination i and upper limits to the stellar masses. The results in each limit are shown in Table 2. The true values of the masses of the component stars within the system may lie anywhere between these limits for corresponding combinations of β and i. In order to determine the uncertainties on each derived parameter, we performed a Monte Carlo analysis which propagated the uncertainties through 10^4 trials, assuming a Guassian distribution in each individual uncertainty.

Between phases $\phi \sim 0.4$ - 0.6 the He I 1.70 μm absorption line displays asymmetric features for a number of the spectra (Fig 1). To investigate the effect these asymmetries have on the final orbital solution, we omitted spectra between this phase range and calculated a new set of NS and donor star masses. We found the impact on the derived orbital solution of these asymmetries to be negligible and have included the full set of measured radial velocities for completeness. We are unsure of the exact physical cause of these asymmetric features, but there appears to be a correlation between the airmass of the observation and the degree of asymmetry observed. We favour atmospheric effects arising at the time of the observation to be the cause; whilst acknowledging that they have a negligible effect upon the calculated system masses.

4. IGR J18027-2016 Spectral classification

The H band spectrum is displayed in Fig. 3(a). Here we see the He I 1.700 μm line is present but there is no detection of He II 1.692 μm, which is seen in absorption in early and late O supergiants and typically absent in early B supergiants. Further spectral indicators include the two hydrogen lines, Brackett 10 (1.736 μm) and Brackett 11 (1.681 μm) which display relatively weak absorption features indicative of B0 - B1 I (Hanson et al. 2005). Examining the K_s band, the absence of lines due to the C IV triplet (2.069, 2.078 and 2.083 μm) combined with the He I 2.058 μm line in emission implies IGR J18027-2016 is not an O type supergiant (Mason et al. 2009). Further constraining the spectral type, we can see that He I 2.058 μm is in emission and when combined with the observed He I 2.112 μm line in absorption, this is indicative of a B0-B2 I classification. The N III 2.115 μm line seen in emission allows us to again converge on a spectral type of B0-B1 I (Hanson et al. 2005).

We can also see that Br γ displays relatively weak emission, unfortunately we have no spectral coverage of the He II 2.189 μm line region. As the spectral features in the K_s band are not highly dependent on luminosity, we have difficulty distinguishing between luminosity sub-classes. We can not localise the classification to any better than B0 - B1 I. This is broadly in agreement with the spectral type found by Torrejón et al. (2010) of B1 Ib. IGR J18027-2016 does not appear to exhibit any secular changes in spectral morphology, both the K band spectrum obtained by Torrejón et al. (2010) and the spectrum shown in Fig. 3(b) are separated by 5 years but are very similar.

5. Conclusions

Within this paper we have presented the analysis and results of multi-epoch observations of the eclipsing high mass X-ray bi-

nary IGR J18027-2016 performed at the ESO/VLT with the NIR spectrograph ISAAC. These have enabled us to make the first measurements of the dynamical masses of both system components. Constructing an orbital solution from near-IR radial velocity measurements and the orbital parameters of the system, provides a dynamically determined neutron star mass of 1.4 ± 0.2 - 1.6 ± 0.3 $M_{\odot}$.

The mass and radius of the supergiant donor, M ~ 18 - 22 $M_{\odot}$ and R ~ 17 - 20 $R_{\odot}$ is in agreement with that suggested from X-ray observations (M ~ 21 $M_{\odot}$, R ~ 19 $R_{\odot}$; Hill et al. (2005)). We find the spectral type of the donor to be B0-B1 I, this is in accord with that found previously (B1 Ib) by Torrejón et al. (2010). Although we note that due to the lack of spectral coverage encompassing the He II 2.189 μm line, this prevented us from conducting non-LTE stellar atmosphere modelling and extracting the full range of stellar parameters. Particularly useful would have been a determination of the stellar temperature that would enable us to accurately constrain the luminosity subclass. From an examination of a sample of Galactic B supergiants (Searle et al. 2008) the donor has a wide possible range of luminosities, $\log(L/L_{\odot})$ ~ 5.5 - 5.7 and temperatures $\log T_{eff}$ ~ 4.3 - 4.5. Comparing this parameter range to evolutionary tracks (Fig. 8 Searle et al. (2008)) leads us to suspect that the donor's progenitor mass was ~ 30 $M_{\odot}$.

Acknowledgements. ABM acknowledges support from an STFC studentship. JSC acknowledges support from an RCUK fellowship. This research is partially supported by grants AYA2008-06166-C03-03 and Consolider-GTC CSD-2006-00070 from the Spanish Ministerio de Ciencia e Innovación (MICINN). Based on observations carried out at the European Southern Observatory, Chile through programme ID 085.D-0539(A).

References

Augello, G., Iaria, R., Robba, N. R., et al. 2003, ApJ, 596, L63
Chaty, S., Rahoui, F., Foellmi, C., et al. 2008, A&A, 484, 783
Demorest, P. B., Pennucci, T., Ransom, S. M., Roberts, M. S. E., & Hessels, J. W. T. 2010, Nature, 467, 1081
Hanson, M. M., Kudritzki, R.-P., Kenworthy, M. A., Puls, J., & Tokunaga, A. T. 2005, ApJS, 161, 154
Hill, A. B., Walter, R., Knigge, C., et al. 2005, A&A, 439, 255
Joss, P. C. & Rappaport, S. A. 1984, ARA&A, 22, 537
Kaper, L., van der Meer, A., van Kerkwijk, M., & van den Heuvel, E. 2006, The Messenger, 126, 27
Masetti, N., Mason, E., Morelli, L., et al. 2008, A&A, 482, 113
Mason, A. B., Clark, J. S., Norton, A. J., et al. 2011, ArXiv e-prints
Mason, A. B., Clark, J. S., Norton, A. J., Negueruela, I., & Roche, P. 2009, A&A, 505, 281
Mason, A. B., Norton, A. J., Clark, J. S., Negueruela, I., & Roche, P. 2010, A&A, 509, A79+
Quaintrell, H., Norton, A. J., Ash, T. D. C., et al. 2003, A&A, 401, 313
Revnivtsev, M. G., Sunyaev, R. A., Varshalovich, D. A., et al. 2004, Astronomy Letters, 30, 382
Searle, S. C., Prinja, R. K., Massa, D., & Ryans, R. 2008, A&A, 481, 777
Torrejón, J. M., Negueruela, I., Smith, D. M., & Harrison, T. E. 2010, A&A, 510, A61+
Walter, R., Zurita Heras, J., Bassani, L., et al. 2006, A&A, 453, 133